ACS Energy LETTERS

http://pubs.acs.org/journal/aelccp

PERSPECTIVE

The Fascinating Properties of Tin-Alloyed Halide Perovskites

Jun Xi and Maria Antonietta Loi*

Cite This: *ACS Energy Lett.* 2021, 6, 1803−1810

Read Online

ACCESS | Metrics & More | Article Recommendations

ABSTRACT: **Tin-alloyed halide perovskites are progressively becoming more popular as slowly their optoelectronic properties start to rival those of the potentially risky pure lead analogues. However, to push this attractive semiconductor toward realistic applications, several major issues need to be solved. This Perspective will start with a description of the fundamental properties of tin-alloyed halide perovskites, continue discussing their weak points with special attention on the structural and electronic instabilities, and conclude examining the effects of the above-mentioned properties on devices. Finally we propose a plausible roadmap to further boost tin-alloyed halide perovskite devices to practical applications. We believe this roadmap should start from an understanding of this family of semiconductors from an atomistic viewpoint, proceeding to the control of thin-film fabrication, the structural properties, and finally the device optimization. We hope this Perspective can help to inject new enthusiasm and facilitate the progress in tin-alloyed halide perovskites, catalyzing their transition from the cradle of the laboratories to the reality of their fabrication.**

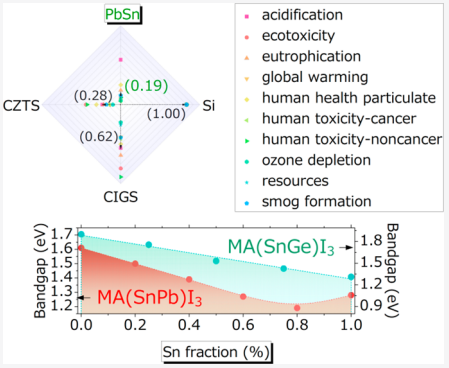

Metal halide perovskites have emerged as a magnificent class of semiconductors for the development of frontier multifunctional devices, especially ones with optoelectronic functionalities.[1,2] Their prospects could be anticipated owing to the low-cost scalable processability and broad window of controllable bandgap.[3] In spite of the surge pushing for superior devices, application-minded scientists and engineers have appealed for reduction or even elimination of the critical metal lead (Pb) within the perovskite lattice, due to regulations around the world on the use of toxic elements in industrial products.[4] The real impact of Pb on human beings as well as on ecosystems raises concerns in different communities.

A recent study has compared the capacity of Pb and Sn coming from metal halide perovskites to penetrate into the food chain through plants.[5] As shown in Figure 1a, the uptake of Pb by mint plants grown in Pb perovskites-contaminated soil (250 mg kg^{-1}) is several orders of magnitude higher than that of plants grown in the natural soil.[5] In addition, the collective uptake ability of Pb increases as the Pb concentration increases (Figure 1b). In contrast, tin (Sn), with the ability to support similar lattice structures, as it is a member of the same chemical group as Pb, appears to be environmentally friendlier than Pb even in high concentrations (Figure 1b). Hence, Sn perovskites are to be considered safer for the environment and human health.

For these reasons, Sn-based perovskites have recently attracted large interest both for their fundamental properties and for device applications.[6−9] In particular, the efficiency of photovoltaic devices using Sn-based perovskites has progressively grown and recently yielded values beyond 10%.[10−14] Although studies on Sn-based perovskites appear to be thriving, the easy oxidization of Sn^{2+} to Sn^{4+} evidently destabilizes the perovskite lattice.[6] More importantly, tin vacancies form naturally during the crystallization or due to the oxidized Sn^{4+}, leading to a strong p-type self-doping of the material, with large consequences for device performance when using a p-i-n or n-i-p structures.[13,15]

However, alloying of Sn with other metals provides unexpected opportunities.[16] Encouragingly, alloys of Sn and Pb perovskites give rise not only to enhanced device efficiency (respect to pure Sn perovskites) but also to increased band gap tunability and structural and environmental stability.[17]

A recent study has pointed out that SnPb perovskites, among different photovoltaic semiconductors, have the lowest environmental impact (Figure 1c).[18] All the merits of SnPb perovskites suggest for them an important position in the

Received: February 8, 2021
Accepted: April 2, 2021
Published: April 14, 2021

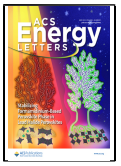

ACS Publications

© 2021 The Authors. Published by American Chemical Society

https://doi.org/10.1021/acsenergylett.1c00289
ACS Energy Lett. 2021, 6, 1803−1810

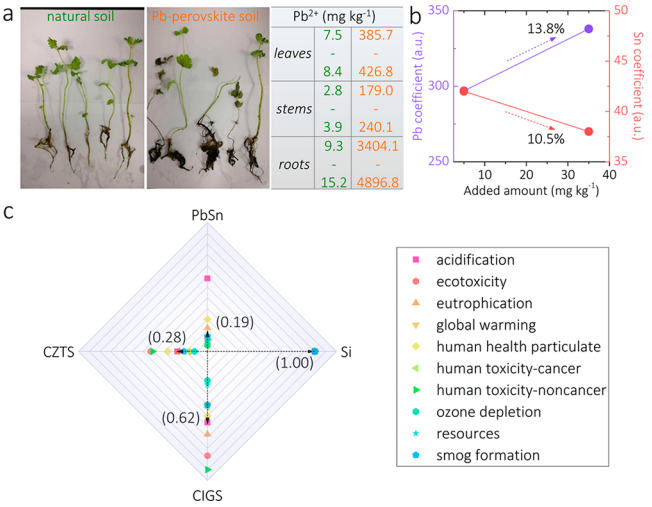

Figure 1. (a) Photographs of mint plants grown on natural soil and 250 mg kg^{-1} Pb^{2+} perovskite-contaminated soil. The table on the right gives the measured Pb^{2+} content in the corresponding position. Reproduced with permission from ref 5. Copyright 2020 The Author(s), published by Springer Nature under a Creative Commons Attribution 4.0 International License (http://creativecommons.org/licenses/by/4.0/). (b) Metal (Pb/Sn) uptake ability as a function of amount of metal added. The data are extracted from ref 5. (c) Environmental impact indicators of single-junction solar cells using different semiconductors, normalized by related parameters of Si cells. The data are taken from ref 18.

future of metal halide perovskite optoelectronic devices. In addition, a peculiar enhanced stability has been observed in tin−germanium (SnGe)-alloyed perovskites.[19] In this Perspective, we will first discuss the origin and dependence of the intrinsic properties and stabilities of the perovskites of alloyed Sn, and then propose the next steps to enhance the properties of such semiconductors.

Any serious discussion on the electronic properties of solids should start with an understanding of their lattice structure. Three-dimensional (3D) metal halide perovskites adopt structures ranging from standard cubic to distorted tetragonal/orthorhombic.[3] In these structures, cations such as methylammonium (MA^+), formamidinium (FA^+), and Cs^+ fill the spaces between octahedrons, while the halide anions (Cl^-, Br^-, and I^-) occupy the octahedron's vertices and a divalent metal is in its center.[3] Interestingly, the low formation enthalpy of perovskites allows the flexible admixture of chemical entities at these sites; namely, they can be alloyed.[20]

Since our intention is to arouse the attention of the optoelectronics research field, in this context we aim to focus on the Sn-alloyed triiodide perovskites which show the narrower band gap among the Pb and Sn perovskites. For a broader discussion on other types of metal halide perovskite, we would like to refer the reader to the recent work of Manna.[21]

It has been underlined that, while the cations in the A position (FA^+, MA^+, and Cs^+) make a negligible contribution to the electronic structure, they can modify the crystalline structure enormously, having an indirect effect on it. In contrast, the nature of the divalent metal is fundamental for the electronic structure, and the band structure near the band edge is dominated by the octahedral units. Irrespective of the metal selection, both the valence band maximum (VBM) and conduction band minimum (CBM) are located at the same position of the Brillouin zone, which defines metal halide perovskites as direct bandgap semiconductors.[21] The nature of the metal can induce also a different degree of spin−orbit coupling (SOC), influencing the bandgap and eventually splitting some of the bands.[23]

In SnPb-alloyed perovskites, the VBM is composed of I *p*-states as well as metal(II) *s*-states, whereas the CBM is almost entirely governed by the metal(II) *p*-states (Figure 2a).[24]

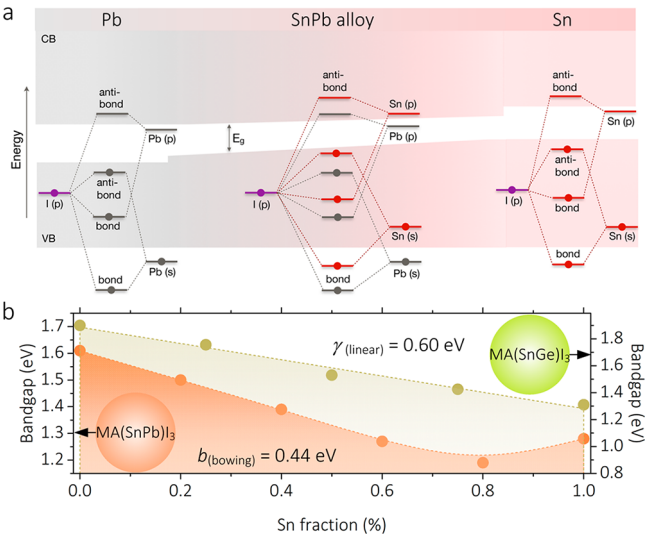

Figure 2. (a) Schematic of band structure of SnPb-alloyed perovskites. Reprinted with permission from ref 24. Copyright 2018 American Chemical Society. (b) Bandgap evolution dependent on Sn fraction in SnPb- and SnGe-alloyed perovskites, respectively. The bowing parameter ($b_{(bowing)}$) in $MASnPbI_3$ perovskite is about 0.44 eV, and the linear parameter ($\gamma_{(bowing)}$) in $MASnGeI_3$ perovskite is about 0.60 eV. The data for $MASnPbI_3$ and $MASnGeI_3$ are extracted from refs 26 and 33.

However, the details differ for pure Pb and Sn perovskites. As for the VBM of pure Pb perovskites, the contributed ratio for I 5*p* appears to be 3 times higher than that of the Pb 6*s* state.[22] Instead, in the case of the pure Sn analogue, the shallower-lying Sn 5*s* state increases the overlap with the I 5*p* orbital, which strongly moves the VBM upward by around 0.7 eV.[25] In terms of the CBM, SOC is a relevant effect, as atom mass scales up from Sn to Pb, where the relative effect on CBM is about 3-fold increased.[24] Hence, the CBM of pure Sn perovskites lies 0.2 eV higher than that of their Pb analogues.[24] However, when looking at the SnPb-alloyed perovskites, the VBM and CBM are not in line with any of the parent compounds. In detail, as the Sn content increases, the alloyed electronic structure becomes more complex. Due to the orbital offsets between Sn and Pb, the VBM of the alloyed material derives from the antibond coupling from Sn 5*s* and I 6*p*, while the pronounced SOC of Pb enables the alloyed CBM to chiefly adopt Pb 6*p* states.[23] Taking MA-based alloy as an example (Figure 2b), a nonlinear dependence of the bandgap on the Sn fraction is presented.[25] This odd, nonlinear shift of the bandgap is known as the bowing effect. It is important to underline that this is not only occurring in MA-based SnPb perovskites, but also alloyed systems using other cations, including FA, Cs, and their mixtures (FAMA, FACs), which display a similar bowing effect with slightly varied bowing parameters.[16,17,27,28] Interestingly, the bowing effect prevails

https://doi.org/10.1021/acsenergylett.1c00289
ACS Energy Lett. 2021, 6, 1803−1810

even in the 2D structures and nanostructures where Sn and Pb are alloyed.[29,30] The benefit of the bowing effect in SnPb-alloyed perovskites is to allow obtaining narrower bandgaps down to 1.2 eV, which is far beyond the values of the pure compounds. Hence, SnPb-alloyed perovskites can provide an opportunity for approaching the Shockley−Queisser (SQ) limit in single-junction solar cells. But even more interestingly, their bandgap is ideal to fabricate bottom sub-cells in fully perovskite tandem solar devices or in combination with another class of materials.[31] In addition, semiconductors of such a bandgap could have applications in night-vision devices and sensors.

SnGe-alloyed perovskites have also been reported; however, at the moment there is very little understanding of these systems.[19] In principle, their electronic structure should resemble that of SnPb-alloyed perovskites.[22] However, the smaller size of Ge forces the elongation of the Ge−I bond, resulting in a weak overlap between the orbitals of the alloyed metals and the I orbitals. Also, the highly distorted $[GeI_3]^-$ blocks are easily formed, breaking the lattice symmetry.[31] In this case, the VBM of SnGe-alloyed perovskites appears to be less dispersive and shifted. Regarding the CBM, Ge 4*p* states have the major contribution.[22] Also, the highly distorted $[GeI_3]^-$ blocks are easily formed breaking the lattice symmetry.[32] Accordingly, in SnGe-alloyed perovskites, the dependence of the bandgap variation on metal fraction does not show the bowing effect but follows a linear trend (Figure 2b).[33] Furthermore, the A cations (FA^+, MA^+, and Cs^+) can modify stereochemically the interaction with Ge 4*s* states, further controlling the bandgap.[34] As it has been reported, Cs-based analogues can be tuned between around 1.3 eV ($CsSnI_3$) and 1.6 eV ($CsGeI_3$), which is in an interesting range for solar cells, light-emitting diodes (LEDs), and photodetectors.[19] However, such alloyed perovskites are seldom reported for applications, probably due to the difficulties in material synthesis and device fabrication.

In view of the electronic structures governed by the mixed chemical bonds, the physical properties of Sn-alloyed perovskites are expectedly largely affected. In fact, the bond interaction and steric arrangement of octahedral blocks greatly correlate to the curvature of the bands with consequences on the electron/hole effective masses,[9] which have a fundamental role determining the transport properties of the systems. Taking SnPb perovskites as an example, higher Sn fractions reduce the tetragonal−orthorhombic phase transition temperature and decrease electron effective masses. When looking at the optical properties of SnPb-alloyed perovskites, the exciton binding energy remains very close to that of the Pb-based compounds, namely around 16 meV, which makes the excitons split promptly at room temperature.[35,36] The lifetimes of charge carriers have been reported to range from the very long one of the parent Pb to the relatively short one of the parent Sn perovskites, with values from about 43 ns up to 200 ns for samples of about 50−50 composition.[37,38] Generally, increasing the Sn ratios is proved to enhance the charge-carrier mobility, as a result of reducing Fröhlich electron−phonon interaction with increasing optical phonon frequencies.[28] However, it is very much dependent on the percentage of alloying, as some studies have pointed out that, for content of Sn between 0.5% and 20%, a defect-rich region is reached with prevailing non-radiative recombination.[28] It is also important to underline that Sn-rich samples do not show excitonic signatures even at very low temperature.[7,9] However, the alloying process should not be taken as an explanation of every physical property. Instead, comprehensive factors such as the number of trap states, the local chemical environment, and the test conditions should be considered carefully before elaborating how the physical properties evolve.

However, the alloying process should not be taken as an explanation of every physical property. Instead, comprehensive factors such as the number of trap states, the local chemical environment, and the test conditions should be considered carefully before elaborating how the physical properties evolve.

Before discussion on the structural stabilities of Sn-alloyed perovskites, a couple of related factors, including the entropy and lattice parameter, are introduced. In principle, for an alloyed crystalline system, the local degree of configurational freedom increases, leading to an enhancement of the mixing entropy and thus, overall, to an enhanced structural stability.[39] The Goldschmidt factor, which gives an indication of the phase stability of a certain perovskite,[40] in the Sn-alloyed phase is insignificantly changed with respect to that of the pure Sn phase, also showing that Sn-alloyed perovskites are thermodynamically stable.

In general, when exposed to ambient conditions, Sn^{2+} is known to be oxidized into Sn^{4+}. The instability problem is notorious for pure Sn perovskites.[13] Surprisingly, Sn-alloyed perovskites show much enhanced stability against air, which is an important factor determining the interest in these systems.

A Sn atom, lacking lanthanide shrinkage, has a smaller ionization energy than Pb, thus more easily losing its valence electrons.[41] Furthermore, the standard reduction potential of Pb^{4+} (+1.67 V) is much larger than that of Sn^{4+} (+0.15 V), showing that Pb^{2+} is more reluctant to be oxidized.[41] The unstable thermodynamic nature of Sn^{2+} can lead to complicated degradation routes, where several triggering factors have been proposed including oxygen, solvents, temperature, light, pressure, etc.[41] Hence, more investigations are needed to identify the factors affecting the degradation mechanism.

However, for SnPb-alloyed solids, the degradation pathway appears to be different due to the local complex coupled Pb−X and Sn−X (X = halide) bonds. The alloyed material is mainly degraded into I_2, SnO_2, and PbI_2, while the pure one is degraded into SnO_2 and SnI_4.[42] This phenomenon stems from the fact that surrounding Pb^{2+} suppresses the presence of multiple adjacent Sn^{2+} interactions, which increases the activation energy for breaking Sn−I bonds from 537 meV for the pure Sn perovskites to 731 meV for the alloyed system.[42] A Pb content of 50% or higher can decrease the degradation rate by orders of magnitude.[42] A recent study has verified by X-ray photoelectron spectroscopy that the degradation product is I_2.[43] More importantly, the authors verified that the degradation is located at the crystal surface, where I_2 is further catalyzed into I_3^- species by uncoordinated I^- anions. On account of I_3^- formation, surface iodide vacancies are created, making the metal under-coordinated (Figure 3a).[43] Such surface-activated degradation is suggested

https://doi.org/10.1021/acsenergylett.1c00289
ACS Energy Lett. 2021, 6, 1803−1810

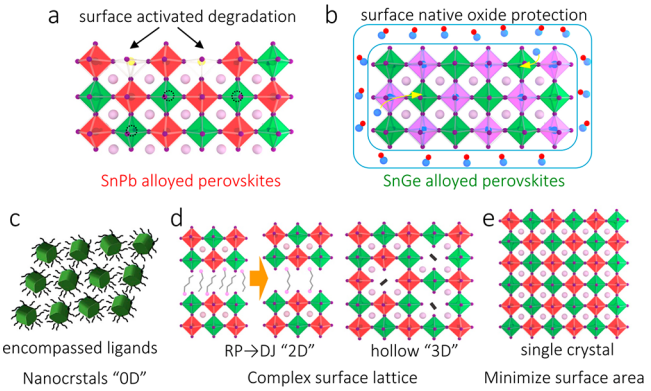

Figure 3. Instability origin of (a) SnPb- and (b) SnGe-alloyed perovskites. Here, the red, green, and purple octahedral units represent $[PbI_6]^{4-}$, $[SnI_6]^{4-}$, and $[GeI_6]^{4-}$, respectively. Dashed circles in (a) denote Sn vacancies. In (b), the shell with blue-red molecules indicates the native oxide surface, and the yellow arrows indicate Ge filling into Sn vacancies. Possible strategies to improve stability involve (c) 0D nanocrystals surrounded with ligands, (d) complex surface lattice with 2D/hollow-3D structure, and (e) minimizing surface area using single crystals.

to occur spontaneously even in inert conditions and can be accelerated in working devices and harsh environments. Interestingly, density functional theory simulations uncovered energetically favored Sn^{2+} oxidation at the crystal surface, in line with the experimental finding.[44] In parallel, formation of Sn^{4+} in bulk is unfavorable, and, when present, Sn^{4+} species undergo spontaneous reduction with the release of a pair of holes in the valence band, leading to formation of Sn vacancies and *p*-doping (Figure 3a).[44] In response to bulk Sn vacancies, surface under-coordinated Sn atoms facilitate Sn^{4+} nucleation. Rationalizing the experimental results and the above-mentioned reaction loop, crystal surfaces should be responsible for the Sn^{2+} oxidation dynamics in SnPb-alloyed perovskites.

For SnGe alloys, stability studies are still at an early stage. Recently, the inorganic $CsSnGeI_3$ has emerged for its stability.[19] An investigation on polycrystalline $CsSnGeI_3$ films revealed the presence of an amorphous Sn-containing Ge^{4+}-rich native oxide (<5 nm) on the film surface, which protects the $CsSnGeI_3$ bulk from oxidation (Figure 3b).[19] Meanwhile, Sn species within the oxide are supposed to block volatile Ge sub-oxides, further reinforcing the lattice of the oxide surface. Another recent study on $CsSnGeI_3$ nanocrystals unveils that the native Sn vacancies can be readily filled by introducing Ge^{2+} to enhance the bulk stability.[45] However, due to the limited knowledge about the chemical composition of surface and bulk, no agreement is reached yet regarding the origin of the improved stability in SnGe-alloyed perovskites.

Considering the current understanding of the factors affecting the stability of Sn-alloyed systems, diverse methods have been proposed to further suppress their degradation, especially on surfaces. The most common state-of-the-art strategies are depicted in Figure 3c: (i) Zero-dimensional colloidal nanocrystals.[45−47] Using rationally designed organic ligands, chemical interactions on crystal surface can be suppressed. Hydrophobic organic ligands anchored to the nanocrystal surface also prevent corrosion by water.[48] (ii) Complex lattices. Assembling low-dimensional (2D) or artificial nanostructure (hollow 3D) close to the crystal surface can significantly change the surface chemistry and formation energy of unwanted species, thus lowering the oxidation rate.[49−52] (iii) Minimizing surface area. Single-crystal or even monocrystalline films, with low surface/bulk ratio, are expected to intrinsically reduce surface activated Sn^{4+} sites and consequently stabilize the crystal.[53] Again, the key idea of these methods lies in the management of the crystal surface, which determines the long-term stability for Sn-alloyed perovskites.

> Again, the key idea of these methods lies in the management of the crystal surface, which determines the long-term stability for Sn-alloyed perovskites.

Owing to the advantages of Sn-alloyed perovskites, we turn now to highlight their applications especially in the optoelectronics field. Here, SnPb perovskites are mostly exploited for their bandgaps (as low as 1.2 eV) which, as discussed above, are ideal for both single-junction and tandem solar cells. Notably, most advanced devices using Sn-alloyed perovskites adopt an inverted structure. In the normal structure, the generally used electron-transporting layers (ETLs) TiO_2, SnO_2, and ZnO do not favor the crystallization of Sn-alloyed perovskites; the rich oxygen interfaces probably also accelerate the oxidization of the Sn sub-lattice.[54] Furthermore, the lithium or cobalt salts used as dopants in the hole-transporting layer (HTL) 2,2′,7,7′-tetrakis(*N*,*N*-di-4-methoxyphenylamino)-9,9′-spiro-bifluorene (Spiro-OMeTAD) and even their acetonitrile solvent can break the weak Sn−X (X = halide) bonds, decomposing the Sn sub-lattice.[54] In addition, the hole-transport ability of Spiro-OMeTAD is generally improved after it is partially oxidized, which however also oxidizes the surfaces of the Sn-based material. Instead, in the inverted structure, no dopants and high-polarity solvents are involved after the active layer deposition, which act as a protection for the Sn sub-lattice. Hence, when this class of perovskite is used as an intrinsic semiconductor, the inverted structure appears more suitable at the moment, at least when limited to HTLs and ETLs generally used for perovskites-based devices.

In Figure 4a we report the evolution of the power conversion efficiencies (PCEs) depending on the bandgap for single-junction and tandem solar cells using alloyed systems. Starting from a PCE of 14.8% in 2016, the SnPb perovskites-based single-junction device underwent lattice tuning, transporting layer optimization, and 2D structure introduction, to reach nowadays, with assistance of a zwitterionic antioxidant, the astonishing PCE of 21.7%.[17,27,37,38,55−59] In a similar fashion, the PCE of the two terminal tandem devices using a SnPb bottom cell has grown from the early 17.0% to reach today 25.6%.[17,37,57−59] Such a swift but brilliant trend made SnPb-alloyed perovskites one of the first candidates to enter in the optoelectronic market.

Recently, a SnGe-alloy-based single-junction solar cell displayed a promising PCE up to 7.11% with relatively good stability, which holds great promise for the future.[19]

While the alloyed systems have gained popularity in solar cells, other applications are lagging behind. A recent work has used SnPb-alloyed perovskites for the fabrication of a NIR LED, showing an external quantum efficiency (EQE) of 5.0%

https://doi.org/10.1021/acsenergylett.1c00289
ACS Energy Lett. 2021, 6, 1803−1810

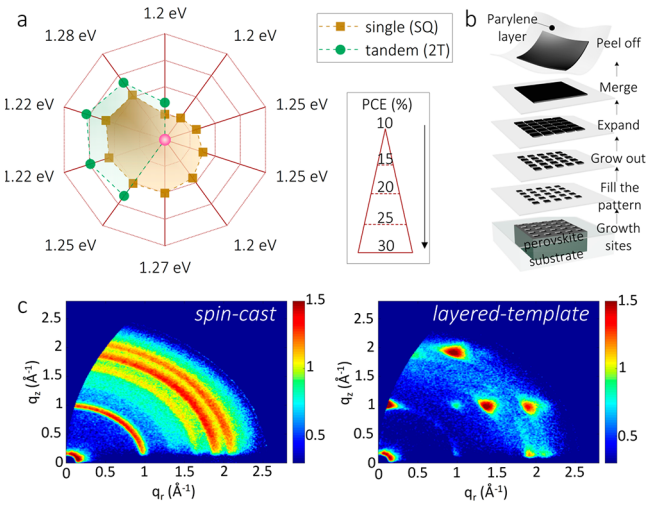

Figure 4. (a) Power conversion efficiency (PCE) progress of single-junction and two-terminal tandem solar cells using SnPb-alloyed perovskites with different bandgaps. (b) Schematic of lithography-assisted epitaxial growth-and-transfer method for single-crystal thin film. Reproduced with permission from ref 53. Copyright 2020, The Author(s), under exclusive licence to Springer Nature Limited. (c) Grazing-incidence wide-angle X-ray scattering (GIWAXS) patterns of spin-casted and layered ($PEA_2Sn_{0.5}Pb_{0.5}I_3$)-templated $FASn_{0.5}Pb_{0.5}I_3$ films from ref 61, submitted for publication 2021.

at 917 nm.[60] To this end, further exploration on improving LEDs based on SnPb-alloyed perovskites can unveil pleasant surprises.

Summary and Outlook. In summary, the research community has witnessed the soaring progress of Sn-alloyed halide perovskites. Better understanding their peculiar electronic structure, deciphering their elusive degradation route, and leveraging their tunable bandgap are of great significance to accelerate the progress in optoelectronics. In spite of the present achievements, the way to practical application still seems long, due to the high complexity of such alloys. There is no doubt that further progress will require coordinated contributions from different fields including physics, chemistry, and engineering. In the following we provide a list of the necessary steps that in our opinion should be undertaken to strengthen the understanding of the properties of Sn-alloyed perovskites and enhance their performance in optoelectronic devices.

Better understanding their peculiar electronic structure, deciphering their elusive degradation route, and leveraging their tunable bandgap are of great significance to accelerate the progress in optoelectronics.

(1) A highly reliable and scalable method of deposition is prerequisite to fabricate Sn-alloyed perovskite-based devices. Highly crystalline and defect-free systems are also fundamental to allow distinguishing intrinsic from extrinsic material properties. Taking the crystal structure and surface-activated degradation into account, a model of a monocrystalline film encapsulated with rationally selected organic ligands/inorganic layer should be highly preferred. Recently, an integrated method of lithography-assisted epitaxial growth and transfer has been proposed to fabricate single crystals of SnPb perovskites with precisely controlled thickness, area, and composition (Figure 4b).[53] Despite the superior quality and stability obtained, the fabrication costs and skills needed make the process rather challenging to implement in large-scale fabrication. Instead, our group has developed a scalable fabrication, which involves the initial deposition by blade-coating of a Ruddlesden−Popper SnPb perovskite as a growth template, which is then converted into $FASnPbI_3$ by an in situ reaction with FAI.[61] The formed film possesses a highly preferred orientation, differing from the spin-cast films of the alloy (Figure 4c). We believe this deposition method will have an important future in the scalable growth of stable Sn-alloyed perovskites.

(2) Optimizing device structure for different Sn-alloyed perovskites is a key to continue improving device performance. Unitl now, most Sn-alloyed perovskites-based optoelectronic devices have adopted similar device structure for Pb perovskites. Although some of them produce superb performances, the distinct electronic band structures as discussed above will limit the charge-carrier extraction/injection efficiency due to the under-considered energy level alignment between active layer and transporting layers. With respect to the solar cells, our group has proposed a polymer-based HTL (PCP-Na) with a suitably matched VB level to suppress both the interface and bulk charge recombination, thus greatly improving device efficiency.[38] Furthermore, it is important to notice the importance of these layers in the deposition of the Sn-alloyed material, as the surface energy of the HTL (or ETL) determines their growth and crystallization. Hence, carefully designed novel organic molecules as well as inorganic compounds are expected to further promote optoelectronic device performance.

(3) Sn-alloyed perovskites-based optoelectronic devices suffer from significant non-radiative recombination due to Sn vacancies, in turn limiting device performances. Hence, efficiently removing or reducing the quantity of Sn vacancies is a key to facilitate Sn alloy device development. Notably, the previous discussion points out that Sn^{4+} formation in bulk has a high probability to induce Sn vacancies and self-p-doping. Therefore, the suppression of Sn^{4+} formation at any stage, namely, in the precursors and during fabrication, storage, and measurements, should be highlighted. Additives such as SnX_2 (X = halide) in low concentrations are known to limit Sn^{2+} oxidization in the precursors.[41] Other strategies such as the addition of reducing agents like Sn^0 and hydrazine, other metal doping, and the use of large organic cations have been used to further mitigate Sn vacancies prior to their formation.[41] After thin-film fabrication, the most diffuse approach has been to protect the Sn-alloyed perovskites from ambient conditions;0 this approach together with the use of highly crystalline films seems the most successful. Recently, we have demonstrated that field effect transistors made with the most sensitive pure Sn-based perovskites can be stored for 20 months in a glovebox with a resulting improvement of the device performance.[62]

(4) A comprehensive investigation of the properties at different length scales is essential to fully understand such alloyed perovskites. So far, most fundamental studies are dedicated to identify the collective properties. However, ideal homogeneous properties cannot be obtained in mixed

https://doi.org/10.1021/acsenergylett.1c00289
ACS Energy Lett. 2021, 6, 1803−1810

compositions.[63] Most likely, the spatial heterogeneities varying from Sn-rich to Sn-deficient domains could entail local inhomogeneities. Accordingly, the focus should be on combining diverse techniques to exactly examine the material structure and correlate the fundamental property with the fine structure from atomistic scale to device scale. In particular, real-time methodologies under careful control can be used to visualize the properties at different scales.

(5) Assessment and critical analysis of the device's operational stability in different environments should be reached for accelerating applications. The difference in chemical sensitivity between surface and bulk and the thermodynamics of phase transition impacts the potential degradation pathways. With respect to realistic devices, the key investigations lie in symmetrically decoupling and integrating the individual roles of sub-structure and test factor. This task requires advanced characterization and simulation tools to validate chemical reaction and physical properties simultaneously.

In conclusion, the current comprehension of Sn-alloyed halide perovskites could appear as too limited to draw a possible future landscape. However, we believe that the above suggested steps are the best possible strategy to progressively exploit such semiconductors. Importantly, leveraging Sn-alloyed halide perovskites to meet industrial optoelectronic criteria cannot lag behind the fundamental investigations on their physical properties. Nonetheless, one should bear in mind that imperfections even in pure compounds can disturb the understanding; it is therefore fundamental to continuously double-check obtained experimental results. At the end, we hope this Perspective not only underlines the critical evolution of Sn-alloyed halide perovskites but also gives motivation to the research community to further work on this fascinating system to deepen our current understanding and advance devices made with them.

AUTHOR INFORMATION

Corresponding Author

Maria Antonietta Loi − *Photophysics and OptoElectronics Group, Zernike Institute for Advanced Materials, University of Groningen, 9747 AG Groningen, The Netherlands;* orcid.org/0000-0002-7985-7431; Email: m.a.loi@rug.nl

Author

Jun Xi − *Photophysics and OptoElectronics Group, Zernike Institute for Advanced Materials, University of Groningen, 9747 AG Groningen, The Netherlands;* orcid.org/0000-0001-6600-4862

Complete contact information is available at: https://pubs.acs.org/10.1021/acsenergylett.1c00289

Notes

The authors declare no competing financial interest.

Biographies

Jun Xi is currently a postdoctoral researcher in the Photophysics and OptoElectronics Group, University of Groningen (The Netherlands). He completed his Ph.D. at Xi'an Jiaotong University, and then worked as a postdoctoral researcher at Seoul National University (South Korea). His research interests range from hybrid material design to electronic device application.

Maria Antonietta Loi is now a full professor in the Zernike Institute for Advanced Materials at the University of Groningen (The Netherlands), where she leads the Photophysics and OptoElectronics Group. Her research interests focus on understanding the new hybrid materials and their physics for optoelectronic applications (more details at https://www.photophysics-optoelectronics.nl/).

ACKNOWLEDGMENTS

This work is supported by the Materials for Sustainability (Mat4Sus) program (739.017.005) of The Netherlands Organization for Scientific Research (NWO). Dr. G. Portale and J. Dong from University of Groningen are kindly acknowledged for the GIWAXS measurements. J.X. also thanks Dr. J. Dai for drawing Figure 3.

REFERENCES

(1) Correa-Baena, J.-P.; Saliba, M.; Buonassisi, T.; Grätzel, M.; Abate, A.; Tress, W.; Hagfeldt, A. Promises and Challenges of Perovskite Solar Cells. *Science* **2017**, *358*, 739−744.

(2) Quan, L. N.; Rand, B. P.; Friend, R. H.; Mhaisalkar, S. G.; Lee, T.-W.; Sargent, E. H. Perovskites for Next-Generation Optical Sources. *Chem. Rev.* **2019**, *119*, 7444−7477.

(3) Jena, A. J.; Kulkarni, A.; Miyasaka, T. Halide Perovskite Photovoltaics. *Chem. Rev.* **2019**, *119*, 3036−3103.

(4) Abate, A. Perovskite Solar Cells Go Lead Free. *Joule* **2017**, *1*, 659−664.

(5) Li, J.; Cao, H.-L.; Jiao, W.-B.; Wang, Q.; Wei, M.; Cantone, I.; Lü, J.; Abate, A. Biological Impact of Lead from Halide Perovskites Reveals the Risk of Introducing a Safe Threshold. *Nat. Commun.* **2020**, *11*, 310.

(6) Hao, F.; Stoumpos, C. C.; Cao, D. H.; Chang, R. P. H.; Kanatzidis, M. G. Lead-free Solid-State Organic-Inorganic Halide Perovskite Solar Cells. *Nat. Photonics* **2014**, *8*, 489−494.

(7) Fang, H.-H.; Adjokatse, S.; Shao, S.; Even, J.; Loi, M. A. Long-Lived Hot-Carrier Light Emission and Large Blue Shift in Formamidinium Tin Triiodide Perovskites. *Nat. Commun.* **2018**, *9*, 243.

(8) Kahmann, S.; Shao, S.; Loi, M. A. Cooling, Scattering, and Recombination-The Role of the Material Quality for the Physics of Tin Halide Perovskites. *Adv. Funct. Mater.* **2019**, *29*, 1902963.

(9) Kahmann, S.; Nazarenko, O.; Shao, S.; Hordiichuk, O.; Kepenekian, M.; Even, J.; Kovalenko, M. V.; Blake, G. R.; Loi, M. A. Negative Thermal Quenching in $FASnI_3$ Perovskite Single Crystals and Thin Films. *ACS Energy Lett.* **2020**, *5*, 2512−2519.

(10) Ke, W.; Stoumpos, C. C.; Zhu, M.; Mao, L.; Spanopoulos, I.; Liu, J.; Kontsevoi, O. Y.; Chen, M.; Sarma, D.; Zhang, Y.; Wasielewski, M. R.; Kanatzidis, M. G. Enhanced Photovoltaic Performance and Stability with a New Type of Hollow 3D Perovskite {en}$FASnI_3$. *Sci. Adv.* **2017**, *3*, e1701293.

(11) Xi, J.; Wu, Z.; Jiao, B.; Dong, H.; Ran, C.; Piao, C.; Lei, T.; Song, T.-B.; Ke, W.; Yokoyama, T.; Hou, X.; Kanatzidis, M. G. Multichannel Interdiffusion Driven $FASnI_3$ Film Formation Using Aqueous Hybrid Salt/Polymer Solutions toward Flexible Lead-Free Perovskite Solar Cells. *Adv. Mater.* **2017**, *29*, 1606964.

(12) Ran, C.; Gao, W.; Li, J.; Xi, J.; Li, L.; Dai, J.; Yang, Y.; Gao, X.; Dong, H.; Jiao, B.; Spanopoulos, I.; Malliakas, C. D.; Hou, X.; Kanatzidis, M. G.; Wu, Z. Conjugated Organic Cations Enable Efficient Self-Healing $FASnI_3$ Solar Cells. *Joule* **2019**, *3*, 3072−3087.

(13) Shao, S.; Liu, J.; Portale, G.; Fang, H.-H.; Blake, G. R.; ten Brink, G. H.; Koster, L. J. A.; Loi, M. A. Highly Reproducible Sn-Based Hybrid Perovskite Solar Cells with 9% Efficiency. *Adv. Energy Mater.* **2018**, *8*, 1702019.

(14) Meng, X.; Wang, Y.; Lin, J.; Liu, X.; He, X.; Barbaud, J.; Wu, T.; Noda, T.; Yang, X.; Han, L. Templated Growth of $FASnI_3$ Crystals for Efficient Tin Perovskite Solar Cells. *Joule* **2020**, *4*, 902−912.

(15) Meggiolaro, D.; Ricciarelli, D.; Alasmari, A. A.; Alasmary, F.A. S.; De Angelis, F. Tin versus Lead Redox Chemistry Modulates Charge Trapping and Self-Doping in Tin/Lead Iodide Perovskites. *J. Phys. Chem. Lett.* **2020**, *11*, 3546−3556.

(16) Hao, F.; Stoumpos, C. C.; Chang, R. P. H.; Kanatzidis, M. G. Anomalous Band Gap Behavior in Mixed Sn and Pb Perovskites Enables Broadening of Absorption Spectrum in Solar Cells. *J. Am. Chem. Soc.* **2014**, *136*, 8094−8099.
(17) Eperon, G. E.; Leijtens, T.; Bush, K. A.; Prasanna, R.; Green, T.; Wang, J. T.-W.; McMeekin, D. P.; Volonakis, G.; Milot, R. L.; May, R.; Palmstrom, A.; Slotcavage, D. J.; Belisle, R. A.; Patel, J. B.; Parrott, E. S.; Sutton, R. J.; Ma, W.; Moghadam, F.; Conings, B.; Babayigit, A.; Boyen, H.-G.; Bent, S.; Giustino, F.; Herz, L. M.; Johnston, M. B.; McGehee, M. D.; Snaith, H. J. Perovskite-Perovskite Tandem Photovoltaics with Optimized Bandgaps. *Science* **2016**, *354*, 861−865.
(18) Celik, I.; Phillips, A. B.; Song, Z.; Yan, Y.; Ellingson, R. J.; Heben, M. J.; Apul, D. Environmental Analysis of Perovskites and Other Relevant Solar Cell Technologies in a Tandem Configuration. *Energy Environ. Sci.* **2017**, *10*, 1874−1884.
(19) Chen, M.; Ju, M.-G.; Garces, H. F.; Carl, A. D.; Ono, L. K.; Hawash, Z.; Zhang, Y.; Shen, T.; Qi, Y.; Grimm, R. L.; Pacifici, D.; Zeng, X. C.; Zhou, Y.; Padture, N. P. Highly Stable and Efficient All-Inorganic Lead-Free Perovskite Solar Cells with Native-Oxide Passivation. *Nat. Commun.* **2019**, *10*, 16.
(20) Gebhardt, J.; Rappe, A. M. Mix and Match: Organic and Inorganic Ions in the Perovskite Lattice. *Adv. Mater.* **2019**, *31*, 1802697.
(21) Akkerman, Q. A.; Manna, L. What Defines a Halide Perovskite? *ACS Energy Lett.* **2020**, *5*, 604−610.
(22) Brenner, T. M.; Egger, D. A.; Kronik, L.; Hodes, G.; Cahen, D. Hybrid Organic−Inorganic Perovskites: Low-Cost Semiconductors with Intriguing Charge-Transport Properties. *Nat. Rev. Mater.* **2016**, *1*, 15007.
(23) Manser, J. S.; Christians, J. A.; Kamat, P. V. Intriguing Optoelectronic Properties of Metal Halide Perovskites. *Chem. Rev.* **2016**, *116*, 12956−13008.
(24) Goyal, A.; McKechnie, S.; Pashov, D.; Tumas, W.; van Schilfgaarde, M.; Stevanović, V. Origin of Pronounced Nonlinear Band Gap Behavior in Lead−Tin Hybrid Perovskite Alloys. *Chem. Mater.* **2018**, *30*, 3920−3928.
(25) Ke, W.; Stoumpos, C. C.; Kanatzidis, M. G. Unleaded" Perovskites: Status Quo and Future Prospects of Tin-Based Perovskite Solar Cells. *Adv. Mater.* **2019**, *31*, 1803230.
(26) Zhao, B.; Abdi-Jalebi, M.; Tabachnyk, M.; Glass, H.; Kamboj, V. S.; Nie, W.; Pearson, A. J.; Puttisong, Y.; Gödel, K. C.; Beere, H. E.; Ritchie, D. A.; Mohite, A. D.; Dutton, S. E.; Friend, R. H.; Sadhanala, A. High Open-Circuit Voltages in Tin-Rich Low-Bandgap Perovskite-Based Planar Heterojunction Photovoltaics. *Adv. Mater.* **2017**, *29*, 1604744.
(27) Liao, W.; Zhao, D.; Yu, Y.; Shrestha, N.; Ghimire, K.; Grice, C. R.; Wang, C.; Xiao, Y.; Cimaroli, A. J.; Ellingson, R. J.; Podraza, N. J.; Zhu, K.; Xiong, R.-G.; Yan, Y. Fabrication of Efficient Low-Bandgap Perovskite Solar Cells by Combining Formamidinium Tin Iodide with Methylammonium Lead Iodide. *J. Am. Chem. Soc.* **2016**, *138*, 12360−12363.
(28) Klug, M. T.; Milot, R. L.; Patel, J. B.; Green, T.; Sansom, H. C.; Farrar, M. D.; Ramadan, A. J.; Martani, S.; Wang, Z.; Wenger, B.; Ball, J. M.; Langshaw, L.; Petrozza, A.; Johnston, M. B.; Herz, L. M.; Snaith, H. J. Metal Composition Influences Optoelectronic Quality in Mixed-Metal Lead−Tin Triiodide Perovskite Solar Absorbers. *Energy Environ. Sci.* **2020**, *13*, 1776−1787.
(29) Lei, T.; Lai, M.; Kong, Q.; Lu, D.; Lee, W.; Dou, L.; Wu, V.; Yu, W.; Yang, P. Electrical and Optical Tunability in All-Inorganic Halide Perovskite Alloy Nanowires. *Nano Lett.* **2018**, *18*, 3538−3542.
(30) Lu, H.; Xiao, C.; Song, R.; Li, T.; Maughan, A. E.; Levin, A.; Brunecky, R.; Berry, J. J.; Mitzi, D. B.; Blum, V.; Beard, M. C. Highly Distorted Chiral Two-Dimensional Tin Iodide Perovskites for Spin Polarized Charge Transport. *J. Am. Chem. Soc.* **2020**, *142*, 13030−1304.
(31) Gu, S.; Lin, R.; Han, Q.; Gao, Y.; Tan, H.; Zhu, J. Tin and Mixed Lead−Tin Halide Perovskite Solar Cells: Progress and their Application in Tandem Solar Cells. *Adv. Mater.* **2020**, *32*, 1907392.
(32) Stoumpos, C. C.; Frazer, L.; Clark, D. J.; Kim, Y. S.; Rhim, S. H.; Freeman, A. J.; Ketterson, J. B.; Jang, J. I.; Kanatzidis, M. G. Hybrid Germanium Iodide Perovskite Semiconductors: Active Lone Pairs, Structural Distortions, Direct and Indirect Energy Gaps, and Strong Nonlinear Optical Properties. *J. Am. Chem. Soc.* **2015**, *137*, 6804−6819.
(33) Nagane, S.; Ghosh, D.; Hoye, R. L. Z.; Zhao, B.; Ahmad, S.; Walker, A. B.; Islam, M. S.; Ogale, S.; Sadhanala, A. Lead-Free Perovskite Semiconductors Based on Germanium−Tin Solid Solutions: Structural and Optoelectronic Properties. *J. Phys. Chem. C* **2018**, *122*, 5940−5947.
(34) Ju, M.-G.; Dai, J.; Ma, L.; Zeng, X. C. Lead-Free Mixed Tin and Germanium Perovskites for Photovoltaic Application. *J. Am. Chem. Soc.* **2017**, *139*, 8038−8043.
(35) Galkowski, K.; Surrente, A.; Baranowski, M.; Zhao, B.; Yang, Z.; Sadhanala, A.; Mackowski, S.; Stranks, S. D.; Plochocka, P. Excitonic Properties of Low-Band-Gap Lead−Tin Halide Perovskites. *ACS Energy Lett.* **2019**, *4*, 615−621.
(36) Fang, H.-H.; Raissa, R.; Abdu-Aguye, M.; Adjokatse, S.; Blake, G. R.; Even, J.; Loi, M. A. Photophysics of Organic−Inorganic Hybrid Lead Iodide Perovskite Single Crystals. *Adv. Funct. Mater.* **2015**, *25*, 2378−2385.
(37) Lin, R.; Xiao, K.; Qin, Z.; Han, Q.; Zhang, C.; Wei, M.; Saidaminov, M. I.; Gao, Y.; Xu, J.; Xiao, M.; Li, A.; Zhu, J.; Sargent, E. H.; Tan, H. Monolithic All-Perovskite Tandem Solar Cells with 24.8% Efficiency Exploiting Comproportionation to Suppress Sn(II) Oxidation in Precursor Ink. *Nat. Energy* **2019**, *4*, 864−873.
(38) Shao, S.; Cui, Y.; Duim, H.; Qiu, X.; Dong, J.; ten Brink, G. H.; Portale, G.; Chiechi, R. C.; Zhang, S.; Hou, J.; Loi, M. A. Enhancing the Performance of the Half Tin and Half Lead Perovskite Solar Cells by Suppression of the Bulk and Interfacial Charge Recombination. *Adv. Mater.* **2018**, *30*, 1803703.
(39) Rakita, Y.; Lubomirsky, I.; Cahen, D. When Defects Become 'Dynamic': Halide Perovskites: A New Window on Materials? *Mater. Horiz.* **2019**, *6*, 1297−1305.
(40) Qian, F.; Hu, M.; Gong, J.; Ge, C.; Zhou, Y.; Guo, J.; Chen, M.; Ge, Z.; Padture, N. P.; Zhou, Y.; Feng, J. Enhanced Thermoelectric Performance in Lead-Free Inorganic CsSn1−xGexI3 Perovskite Semiconductors. *J. Phys. Chem. C* **2020**, *124*, 11749−11753.
(41) Awais, M.; Kirsch, R. L.; Yeddu, V.; Saidaminov, M. I. Tin Halide Perovskites Going Forward: Frost Diagrams Offer Hints. *ACS Materials Lett.* **2021**, *3*, 299−307.
(42) Leijtens, T.; Prasanna, R.; Gold-Parker, A.; Toney, M. F.; McGehee, M. D. Mechanism of Tin Oxidation and Stabilization by Lead Substitution in Tin Halide Perovskites. *ACS Energy Lett.* **2017**, *2*, 2159−2165.
(43) Mundt, L. E.; Tong, J.; Palmstrom, A. F.; Dunfield, S. P.; Zhu, K.; Berry, J. J.; Schelhas, L. T.; Ratcliff, E. L. Surface-Activated Corrosion in Tin−Lead Halide Perovskite Solar Cells. *ACS Energy Lett.* **2020**, *5*, 3344−3351.
(44) Ricciarelli, D.; Meggiolaro, D.; Ambrosio, F.; De Angelis, F. Instability of Tin Iodide Perovskites Bulk p-Doping versus Surface Tin Oxidation. *ACS Energy Lett.* **2020**, *5*, 2787−2795.
(45) Liu, M.; Pasanen, H.; Ali-Löytty, H.; Hiltunen, A.; Lahtonen, K.; Qudsia, S.; Smått, J.-H.; Valden, M.; Tkachenko, N. V.; Vivo, P. B-Site Co-Alloying with Germanium Improves the Efficiency and Stability of All-Inorganic Tin-Based Perovskite Nanocrystal Solar Cells. *Angew. Chem., Int. Ed.* **2020**, *59*, 22117−22125.
(46) Liu, F.; Ding, C.; Zhang, Y.; Ripolles, T. S.; Kamisaka, T.; Toyoda, T.; Hayase, S.; Minemoto, T.; Yoshino, K.; Dai, S.; Yanagida, M.; Noguchi, H.; Shen, Q. Colloidal Synthesis of Air-Stable Alloyed $CsSn_{1-x}Pb_xI_3$ Perovskite Nanocrystals for Use in Solar Cells. *J. Am. Chem. Soc.* **2017**, *139*, 16708−16719.
(47) Liu, F.; Jiang, J.; Zhang, Y.; Ding, C.; Toyoda, T.; Hayase, S.; Wang, R.; Tao, S.; Shen, Q. Near-Infrared Emission from Tin−Lead (Sn−Pb) Alloyed Perovskite Quantum Dots by Sodium Doping. *Angew. Chem., Int. Ed.* **2020**, *59*, 8421−8424.
(48) Xi, J.; Piao, C.; Byeon, J.; Yoon, J.; Wu, Z.; Choi, M. Rational Core−Shell Design of Open Air Low Temperature In Situ

https://doi.org/10.1021/acsenergylett.1c00289
ACS Energy Lett. 2021, 6, 1803−1810

Processable $CsPbI_3$ Quasi-Nanocrystals for Stabilized p-i-n Solar Cells. *Adv. Energy Mater.* **2019**, *9*, 1901787.
(49) Ramirez, D.; Schutt, K.; Wang, Z.; Pearson, A. J.; Ruggeri, E.; Snaith, H. J.; Stranks, S. D.; Jaramillo, F. Layered Mixed Tin−Lead Hybrid Perovskite Solar Cells with High Stability. *ACS Energy Lett.* **2018**, *3*, 2246−2251.
(50) Spanopoulos, I.; Ke, W.; Stoumpos, C. C.; Schueller, E. C.; Kontsevoi, O. Y.; Seshadri, R.; Kanatzidis, M. G. Unraveling the Chemical Nature of the 3D "Hollow" Hybrid Halide Perovskites. *J. Am. Chem. Soc.* **2018**, *140*, 5728−5742.
(51) Xi, J.; Spanopoulos, I.; Bang, K.; Xu, J.; Dong, H.; Yang, Y.; Malliakas, C. D.; Hoffman, J. M.; Kanatzidis, M. G.; Wu, Z. Alternative Organic Spacers for More Efficient Perovskite Solar Cells Containing Ruddlesden−Popper Phases. *J. Am. Chem. Soc.* **2020**, *142*, 19705−19714.
(52) Ke, W.; Chen, C.; Spanopoulos, I.; Mao, L.; Hadar, I.; Li, X.; Hoffman, J. M.; Song, Z.; Yan, Y.; Kanatzidis, M. G. Narrow-Bandgap Mixed Lead/Tin-Based 2D Dion−Jacobson Perovskites Boost the Performance of Solar Cells. *J. Am. Chem. Soc.* **2020**, *142*, 15049−15057.
(53) Lei, Y.; Chen, Y.; Zhang, R.; Li, Y.; Yan, Q.; Lee, S.; Yu, Y.; Tsai, H.; Choi, W.; Wang, K.; Luo, Y.; Gu, Y.; Zheng, X.; Wang, C.; Wang, C.; Hu, H.; Li, Y.; Qi, B.; Lin, M.; Zhang, Z.; Dayeh, S. A.; Pharr, M.; Fenning, D. P.; Lo, Y.-H.; Luo, J.; Yang, K.; Yoo, J.; Nie, W.; Xu, S. A Fabrication Process for Flexible Single-Crystal Perovskite Devices. *Nature* **2020**, *583*, 790−795.
(54) Diau, E. W.-G.; Jokar, E.; Rameez, M. Strategies To Improve Performance and Stability for Tin-Based Perovskite Solar Cells. *ACS Energy Lett.* **2019**, *4*, 1930−1937.
(55) Kapil, G.; Ripolles, T. S.; Hamada, K.; Ogomi, Y.; Bessho, T.; Kinoshita, T.; Chantana, J.; Yoshino, K.; Shen, Q.; Toyoda, T.; Minemoto, T.; Murakami, T. N.; Segawa, H.; Hayase, S. Highly Efficient 17.6% Tin−Lead Mixed Perovskite Solar Cells Realized through Spike Structure. *Nano Lett.* **2018**, *18*, 3600−3607.
(56) Wei, M.; Xiao, K.; Walters, G.; Lin, R.; Zhao, Y.; Saidaminov, M. I.; Todorović, P.; Johnston, A.; Huang, Z.; Chen, H.; Li, A.; Zhu, J.; Yang, Z.; Wang, Y.-K.; Proppe, A. H.; Kelley, S. O.; Hou, Y.; Voznyy, O.; Tan, H.; Sargent, E. H. Combining Efficiency and Stability in Mixed Tin−Lead Perovskite Solar Cells by Capping Grains with an Ultrathin 2D Layer. *Adv. Mater.* **2020**, *32*, 1907058.
(57) Tong, J.; Song, Z.; Kim, D. H.; Chen, X.; Chen, C.; Palmstrom, A. F.; Ndione, P. F.; Reese, M. O.; Dunfield, S. P.; Reid, O. G.; Liu, J.; Zhang, F.; Harvey, S. P.; Li, Z.; Christensen, S. T.; Teeter, G.; Zhao, D.; Al-Jassim, M. M.; van Hest, M. F. A. M.; Beard, M. C.; Shaheen, S. E.; Berry, J. J.; Yan, Y.; Zhu, K. Carrier Lifetimes of > 1 μs in Sn-Pb Perovskites Enable Efficient All-Perovskite Tandem Solar Cells. *Science* **2019**, *364*, 475−479.
(58) Xiao, K.; Lin, R.; Han, Q.; Hou, Y.; Qin, Z.; Nguyen, H. T.; Wen, J.; Wei, M.; Yeddu, V.; Saidaminov, M. I.; Gao, Y.; Luo, X.; Wang, Y.; Gao, H.; Zhang, C.; Xu, J.; Zhu, J.; Sargent, E. H.; Tan, H. All-Perovskite Tandem Solar Cells with 24.2% Certified Efficiency and Area over 1 cm^2 Using Surface-Anchoring Zwitterionic Antioxidant. *Nat. Energy* **2020**, *5*, 870−880.
(59) Li, C.; Song, Z.; Chen, C.; Xiao, C.; Subedi, B.; Harvey, S. P.; Shrestha, N.; Subedi, K. K.; Chen, L.; Liu, D.; Li, Y.; Kim, Y.-W.; Jiang, C.-s.; Heben, M. J.; Zhao, D.; Ellingson, R. J.; Podraza, N. J.; Al-Jassim, M.; Yan, Y. Low-Bandgap Mixed Tin−Lead Iodide Perovskites with Reduced Methylammonium for Simultaneous Enhancement of Solar Cell Efficiency and Stability. *Nat. Energy* **2020**, *5*, 768−776.
(60) Qiu, W.; Xiao, Z.; Roh, K.; Noel, N. K.; Shapiro, A.; Heremans, P.; Rand, B. P. Mixed Lead−Tin Halide Perovskites for Efficient and Wavelength-Tunable Near-Infrared Light-Emitting Diodes. *Adv. Mater.* **2019**, *31*, 1806105.
(61) Xi, J.; Duim, H.; Pitaro, M.; Gahlot, K.; Dong, J.; Portale, G.; Loi, M. A. Scalable Template Driven Formation of Highly Crystalline Lead-Tin Halide Perovskite Films, submitted, 2021.
(62) Shao, S.; Talsma, W.; Pitaro, M.; Dong, J.; Kahmann, S.; Rommens, A. J.; Portale, G.; Loi, M. A. Field-Effect Transistors Based on Formamidinium Tin Triiodide Perovskite. *Adv. Funct. Mater.* **2021**, *31*, 2008478.
(63) Tennyson, E. M.; Doherty, T. A. S.; Stranks, S. D. Heterogeneity at Multiple Length Scales in Halide Perovskite Semiconductors. *Nat. Rev. Mater.* **2019**, *4*, 573−587.

https://doi.org/10.1021/acsenergylett.1c00289
ACS Energy Lett. 2021, 6, 1803−1810